2010

Incorporating a Frost Growth Model with Segment by Segment Heat Exchanger Simulation – Application to Microchannel Heat Exchanger

Sankaranarayanan Padhmanabhan
Oklahoma State University

Daniel Fisher
Oklahoma State University

Lorenzo Cremaschi
Oklahoma State University

Incorporating a Frost Growth Model with Segment by Segment Heat Exchanger Simulation – Application to Microchannel Heat Exchanger

Sankar Padhmanabhan[1]*, Daniel. E. Fisher[1], Lorenzo Cremaschi[1]

[1]School of Mechanical & Aerospace Engineering, Oklahoma State University, Stillwater, OK - 74078
Ph: (405)744-5900
Fax: (405)744-7873
Email: sankar.padhmanabhan@okstate.edu

ABSTRACT

A transient frost model based on scaling approach is developed which can be applied to microchannel heat exchangers. The model is able to predict the thickness of the frost layer and the mass accumulation. The model is also capable of handling the air redistribution that occurs on outdoor coils where frost develops non-uniformly. The frost model is integrated with a segment-by-segment heat exchanger calculation algorithm and is validated against experimental data for different entering fluid temperatures. Model results are compared to measured values of frost thickness and are found to match well for all the cases. Model prediction and experimental measurements both showed that frost grows faster when the temperature is lower. Ignoring the phenomenon of air redistribution was found to result in significant errors in predicted coil capacity. The rate of capacity drop in a microchannel heat exchanger during frosting is high and almost linear through out the period. The rate also increased as the temperature of surface was lowered. In order to solve the redistribution to a greater accuracy, effect of geometry of frost layer in the direction of air flow need to be considered.

1. INTRODUCTION

Microchannel heat exchangers are quickly replacing the conventional bulky fin-and-tube heat exchangers due to their high heat transfer effectiveness. For a desired capacity, a microchannel heat exchanger is smaller in size than a fin-and-tube heat exchanger, resulting in less cost to the manufacturer. While microchannel heat exchangers have become standard choice in automotive applications their use as outdoor coils in heat pumps are still limited. This is due to the fact that microchannel heat exchangers used as outdoor coils frost up faster than conventional fin-tube heat exchangers in winter conditions.

Numerous studies have been reported in the literature focusing on frost and defrost heat transfer performance of fin-tube heat exchangers. Even though microchannels are gaining popularity, very few studies are reported about the frost growth on microchannel heat exchangers. Kim and Groll (2003) reported a comparison between microchannel and fin-and-tube heat exchangers when used as an outdoor coil in a heat pump system. The study included both cooling and heating tests. The authors reported frosting/defrosting time and the heating capacity of the heat pump with both coils. Effect of other variables such as heat exchanger inclination, and fins per inch (FPI) were also studied. The authors concluded that microchannel heat exchangers have a shorter frosting time compared to fin-and-tube heat exchangers, and the time decreased even further with each cycle due to residual water retained at the end of each defrost cycle. The work by Kim and Groll focused on the comparison of frosting times and heating performance but their study did not provide sufficient information on frost growth rate and frost build up on microchannel heat exchangers. Xia et al. (2006) studied the performance of a flat-tube heat exchanger with louvered fins in frosting conditions, which resembles a microchannel heat exchanger. An overall heat transfer coefficient was obtained for the heat exchanger using the experimental temperatures and flow rate. Frost thickness was measured using images by a CCD camera, and frost weight was obtained by using a high precision scale. Xia et al. developed a numerical model, which was also experimentally validated, to predict the frost thickness and blockage ratio. Shao et al. (2010) studied the performance of a packaged heat pump (~30 tons) with microchannel and fin-tube heat exchangers. They presented a frost growth model and compared the simulation results (system capacity and COP) with the experimentally measured values. However their model was not fully validated at coil level and it did not consider the air side effects of frost growth.

The work related to modeling the frost growth on microchannel heat exchangers has been very limited. In order to effectively use the microchannels in outdoor coils of heat pumps, it is important that a frost model be available to engineers to help them study the impact on whole system performance. A model based on scaling approach which was proposed by Storey and Jacobi (1999), is modified and used here to simulate frost growth on microchannel heat exchangers. The model is integrated with a segment-by-segment heat exchanger algorithm to study the local variations in frost growth. In microchannel heat exchangers used as outdoor coils, the frost growth can be highly non-uniform (Kim and Groll, 2003; Padhmanabhan et al., 2008) due to the variations of the local refrigerant temperature and local air velocity. This results in a spatial non-uniformity of the frost growth which yields to subsequent redistribution of air on the frontal face of the coil. The knowledge of local frost growth across the heat exchanger is used to determine the changes in the instantaneous air flow rate across the coil. As time progresses, frost continues to grow and ultimately blocks the coil while the air stream simultaneously redistributes itself toward the less resistant sections and in the end decreases. The model will benefit design engineers in studying the performance of the heat exchanger during frost growth by considering various air side and refrigerant side effects. Results obtained from the model are validated against experimental results. Limitations and improvements to the current model are also discussed.

2. THEORETICAL DEVELOPMENT OF MODEL

2.1 Validity of Quasi-Steady Assumption

The problem of frost growth is a transient problem with combined heat and mass transfer. The situation is further complicated by the moving frost boundary. Previous researchers (Kondepudi and O'Neal, 1993; Lee et al., 1997; Yang et al., 2006) have modeled frost growth as a quasi steady state phenomenon. However the supporting basis for such an assumption is not available in the literature. A theoretical analysis of the governing equations is presented and a condition for validity of steady state assumption is derived in this section. The solution domain that is considered is shown in Figure 1. The following assumptions are made in the development of the equations below:

- Local density variations inside the frost layer can be neglected and the whole frost layer can be represented by average properties.
- The frost layer thickness does not increase when the surface temperature reaches the triple point temperature of water

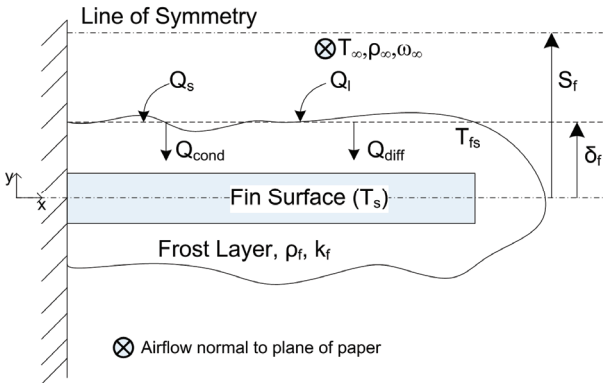

Figure 1: Schematic of Solution Domain for Frost Growth with Associated Heat and Mass Transfer Paths

Applying an energy balance per unit area of the frost layer and considering an energy storage term, we get:

$$k_f\left(\frac{\partial T}{\partial y}\right)_0 = \dot{Q}_s + \dot{Q}_l - \dot{Q}_{stored} \tag{1}$$

The rate of latent energy released due to freezing is equal to the rate of increase in the frost mass and can be represented as

$$\dot{Q}_l = h_{sg}\frac{d\dot{m}_f}{dt} \tag{2}$$

The mass of frost inside the frost layer is equal to the product of the frost density and the frost volume. From the previous assumption of equivalent average frost density and considering a unit area, the rate of latent energy is

$$\dot{Q}_l = h_{sg}\overline{\rho}_f \frac{d\delta_f}{dt} + h_{sg}\delta_f \frac{d\overline{\rho}_f}{dt} \tag{3}$$

Applying (3) in (1) and using standard definitions for sensible heat transfer and energy storage we can rewrite the energy balance as

$$k_f\left(\frac{\partial T}{\partial y}\right)_0 = h(T_\infty - T_{fs}) + h_{sg}\overline{\rho}_f \frac{d\delta_f}{dt} + h_{sg}\delta_f \frac{d\overline{\rho}_f}{dt} - \overline{\rho}_f C_{p,f}\delta_f \frac{\partial T}{\partial t} \tag{4}$$

The energy balance equation can be non-dimensionalized using the dimensionless parameters as shown below. Selection of the triple point of water as the scaling parameter seems logical since the frost surface cannot go beyond that temperature without melting/ refreezing.

$$\theta = \frac{T - T_{tp}}{T_s - T_{tp}} \qquad \delta^x = \frac{\delta_f}{S_f}$$

$$Y = \frac{y}{S_f} \qquad \rho^x = \frac{\rho_f}{\rho_i}$$

Incorporating these dimensionless parameters into the energy balance and rearranging the terms we get the final equation as

$$\left(\frac{\partial\theta}{\partial Y}\right)_0 = \frac{\rho_i h_{sg} S_f^2}{k_f \Delta T}\rho^x \frac{d\delta^x}{dt} + \frac{\rho_i h_{sg} S_f^2}{k_f \Delta T}\delta^x \frac{d\rho^x}{dt} - \frac{\rho_f C_{p,f} S_f^2}{k_f}\delta^x \frac{d\theta}{dt} + \frac{hS_f}{k_f}\left(\frac{T_s - T_\infty}{\Delta T}\right) \tag{5}$$

Where the temperature difference $\Delta T = \left|T_s - T_{tp}\right|$

Equation (5) is the final scaled form of the energy balance in the frost layer, and it can be seen that there are two time constants in the equation. One time constant is related to the rate of change in frost thickness and density (t_{c1}) while the other time constant refers to the rate of change in temperature (t_{c2}). These two time constants are obtained from the equation as follows

$$t_{c1} = \frac{\rho_i h_{sg} S_f^2}{k_f \Delta T} \quad \text{and} \quad t_{c2} = \frac{\rho_f C_{p,f} S_f^2}{k_f}$$

An order of magnitude approach is used to check the conditions when the validity of quasi steady state assumption is valid. For the assumption of quasi-steady state to be valid we require $t_{c1} >> t_{c2}$. Physically, this condition means that the temperature field inside the frost layer stabilizes more quickly than the density and thickness of frost layer as a response to a change in boundary conditions. With the values of the time constants evaluated above and rearranging we get, for a valid quasi steady state assumption

$$\frac{\rho_f C_{p,f}\Delta T}{\rho_i h_{sg}} << 1$$

The dimensionless quantity that arises can be identified as the Jakob number. Thus for a valid quasi steady state assumption in problems similar to frost growth we require

$$Ja << 1 \tag{6}$$

For heat pump applications the frost growth on outdoor coils will always obey this condition. This is due to the fact that in heat pump applications the difference between the plate temperature and the triple point of water is not significant enough to compensate for a low ratio of specific heat to latent energy of sublimation. In some cryogenic applications, where surface temperature is well below sub-freezing temperature, the condition of Eq (6) might not be valid and a quasi steady assumption becomes invalid.

2.2 Frost Model

The governing equations for frost growth are quite complex and even though a quasi steady state assumption allowed a significant simplification and saving in the computational cost, the equations are not provide any closed

form solutions. This is due to the inherent non linearity introduced by the time rate of change of frost density and frost boundaries. For analyzing heat exchangers only average frost layer properties need to be determined. For such conditions the analysis can be simplified further by a scaling approach. One such approach was originally presented by Storey and Jacobi (1999). The model presented here is based on Storey and Jacobi's approach and further improves some aspects of it by removing few more constraints.

One improvement in the current model is to account for the part of water vapor transferred from air which diffuses into frost layer. Another important improvement from the previous model is to account for varying heat and mass transfer coefficients during frost growth. The following assumptions are used for the model:

1. The frost model is quasi-steady state. All variables are constant over an entire time step and no energy is stored in the frost layer during a timestep. The basis for this assumption is given in the previous section.
2. Frost growth is one dimensional. Frost grows only in the direction perpendicular to the air flow.
3. The analogy between heat and mass transfer coefficients exist. This assumption allows us to represent the mass transfer coefficient in terms of heat transfer coefficient.
4. Temperature variation inside the frost layer is linear. This allows scaling the temperature gradient over the whole frost layer.
5. Air inside the frost layer is saturated at the local frost temperature. This allows us to use the Clausius-Clapeyron relation to express vapor pressure in terms of frost temperature.

The model used here is described in detail by Padhmanabhan (2010). Following a similar method and applying an energy balance at the frost surface shown in Figure 1, we see that the heat conducted through the frost layer must be equal to the sum of the sensible heat transfer from the air to the frost surface and the latent heat transfer due to sublimation of water vapor at the frost surface. Equation (7) shows the energy balance applied at the frost surface

$$k_f \frac{\partial T_f}{\partial y} = h(T_\infty - T_{fs}) + \left[h_m(\rho_\infty - \rho_{fs}) - \mathrm{M}\frac{\partial T_f}{\partial y} \right] h_{sg} \tag{7}$$

Where the portion of vapor increasing the density is obtained by using the formulation given by O'Neal (1982)

and $M = D_{AB} \left[\frac{1-\left(\rho_f/\rho_i\right)}{1+\left(\rho_f/\rho_i\right)^{0.5}} \right] \frac{p_v}{RT_{sat}^2} \left(\frac{h_{sg}}{RT_{sat}} - 1 \right)$

Following the scaling approach described by Storey and Jacobi (1999) and relaxing the assumption of constant transfer coefficients, the final form of the energy balance equation in terms of discretized temperature and density differences is shown as follows:

$$k_f \frac{\Delta T_f}{\delta_f} = h\Delta T_\infty + \left[h_m \Delta\rho_\infty - M\frac{\Delta T_f}{\delta_f} \right] h_{sg} \tag{8}$$

Average frost density is calculated as the total frost mass per unit volume of frost. It is thus expressed as

$$\rho_f = \frac{\int_0^t h_m \, \Delta\rho_v \, dt}{\delta_f} \tag{9}$$

The heat and mass transfer analogy is used to express the mass transfer coefficient in terms of the heat transfer coefficient. An appropriate heat transfer correlation is used to relate the heat transfer coefficient to frost thickness by varying fin and tube area. An empirical correlation proposed by Hayashi et al. (1977) is used to calculate density while a correlation proposed by Van Dusen [Saito and Tokura 1991)] is used to calculate frost conductivity.

$$\begin{aligned} \rho_f &= 670 e^{0.277 T_{fs}} \\ k_f &= 0.0209 + 0.403\times10^{-4}\rho_f + 2.37\times10^{-9}\rho_f^3 \end{aligned} \tag{10}$$

Equations (8) - (10) along with an appropriate heat transfer correlation represent a closed system of equations. When the surface temperature is not held constant an additional equation for tube heat balance as shown in Eq. (11) must be introduced to solve for fin and tube surface temperatures. The system can be solved with any non-linear system solver for any time step with air and refrigerant temperature as inputs.

$$h_i A_i\left(T_S - T_{fl}\right) = hA_o\left(T_\infty - T_{fs}\right) + h_m A_o\left(\rho_\infty - \rho_{fs}\right)h_{sg} \tag{11}$$

3. MODEL IMPLEMENTATION

The model developed in the previous section was implemented in FORTRAN for a stand alone microchannel heat exchanger. The geometry and details of the coil used in simulation are given in Table 1. A detailed description of the model implementation is given by Padhmanabhan (2010). Ethylene glycol was used as the fluid inside the heat exchanger and the flow rate was controlled such that the temperature rise from inlet to outlet of the heat exchanger tube is less than 2^0C. The segment by segment heat exchanger simulation is implemented by dividing each tube into 5 segments in the direction of glycol flow i.e. from the bottom to the top of the heat exchanger. Correlations suggested by Kim and Bullard (2002) are used to determine the air side heat transfer coefficient and the friction factor. The total air flow rate on the face of the coil is allowed to drop as the frost grows in order to simulate the real world scenario of heat pumps using a constant speed outdoor fan. The air flow rate on the face of the coil is imposed as a time dependant boundary condition generated from the experiments described in a companion paper (Moallem et al., 2010).

Table 1: Geometry and Related Parameters for the Test Coil

Microchannel Coil Parameter	Value
Coil Face Area (L x W) [m^2]	0.093 (0.3048 x 0.3048)
Tube Orientation	Vertical
Single Tube Length [mm]	304.8
Tube Depth [mm]	25.4
Tube Height [mm]	1.75
Tube Spacing [mm]	9.32
Fin Pitch [fins/m]	787
Fin Thickness [mm]	0.095
Tube/ Fin material	Aluminum/ Aluminum
Number of ports/Geometry	4/Rectangular

4. RESULTS AND DISCUSSIONS

The model presented in the previous section is used to simulate the frost growth on a microchannel at three different entering glycol temperatures (-12.2^{0}C, -9.4^{0}C, -6.7^{0}C). Various parameters such as frost thickness, frost surface temperature and coil capacity are investigated. The boundary conditions for the simulation are the temperatures and flow rates of air and glycol. While the air and fluid temperatures and ethylene glycol flow rate remain constant, the total air flow rate varies through out the simulation to replicate the conditions in the experimental setup presented in Moallem et al (2010). Air Flow rate for all cases at the start of the frosting cycle is 0.09 m^3/s and the frosting period is considered to be finished when the total air flow rate drops below 0.07m^3/s. It is well established that the frost growth is not related to the fluid temperature but is dependent on the surface temperature. On the other hand, the fluid entering temperatures (refrigerant and air) are rather constant and well defined throughout the frosting process. Thus, for clarity in plots and for consistency during the comparison with the actual operating parameters of the outdoor coils, the glycol entering temperature and air approaching temperature are chosen as parameters. Fin surface temperature is a derived variable from the heat and mass balance equations. The results are presented in non-dimensional form whenever such a presentation is reasonable.

Frost thickness at different times for different fluid entering temperatures is shown in Figure 2. The values are normalized based on the half fin spacing. Thickness values obtained from experiments are also plotted in the figure.

Measured thickness match simulated results very well. All three cases end up with similar the same frost thickness. This is as expected since the frost growth is terminated when the air flow rate drops to a 25% of initial value (dry coil). Since the fan curve is constant for all the three cases the final frost thickness is expected to be approximately same. The model currently assumes uniform frost distribution through the depth of the coil which is not the case in real life applications. It needs to be understood that in real conditions lower temperatures cause the frost to be deposited at a significantly higher rate on the front face of the coil thereby resulting in an orifice like condition which causes higher pressure drop. The model does not currently take into account this variation in geometry. Improvement to the model to correctly account the variation in frost thickness in the direction of air flow and thereby its effect on pressure drop is currently underway.

Figure 3 shows the frost surface temperature obtained from the simulations for the three different entering temperature cases. The sharp increase in frost surface temperature and frost thickness for the low temperature case suggests that in such conditions the fin spacing is quickly covered by low density (fluffy) frost which blocks the airflow. At the end of cycle, the weight of frost deposited on low temperature surfaces will be less than the weight of frost deposited on high temperature surfaces. The variation of frost surface temperature is significantly less for the highest temperature case.

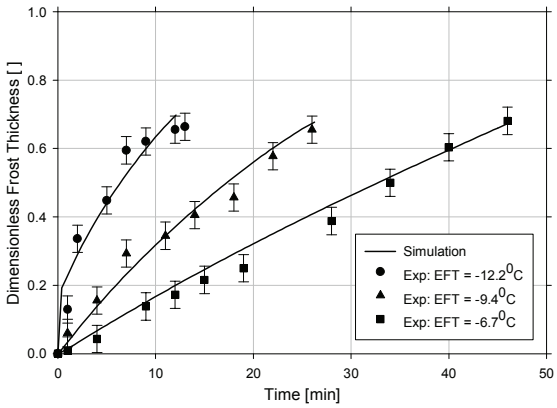

Figure 2: Experimental and Simulated Frost Thickness for Different Entering Glycol Temperatures.

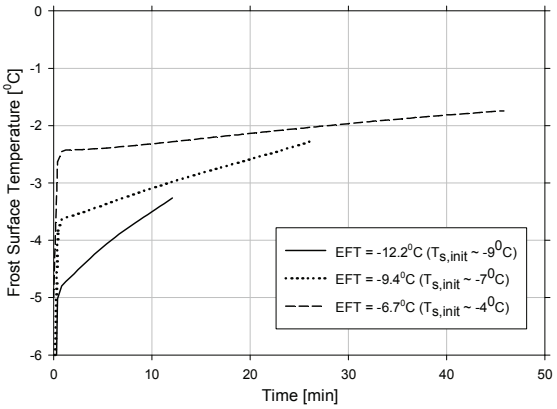

Figure 3: Frost Surface Temperature at First Segment for Different Entering Glycol Temperatures (Approx. Initial Fin Temperatures shown in parenthesis)

Air redistribution that occurs on the face of the heat exchanger is one of the most important aspects of this study. Figure 4 shows the frost thickness for 5 different segments for -9.4^{0}C inlet fluid temperature case. The frost grows faster in segments near the inlet header (upstream) compared to later segments (downstream). Figure 5 shows the variation of air flow through each segment presented as a normalized mass flux. Mass flux through each segment at any time is divided by the initial mass flux through that segment to obtain the normalized parameter. It can be seen from the figure that the mass flux through the segments varies continuously throughout the frosting period. While the mass flux decreases for segments with thicker frost (segments 1 & 2), the flow redistributes itself to less thick (low resistance) segments (segments 4 & 5). It is important to capture this redistribution of the air flow because in actual heat pump units microchannels are sized as condensers and will be oversized when used as evaporators in winter. The non-uniformity in frost growth in microchannels used as out door coils in heat pumps is confirmed in literature (Kim and Groll, 2003; Padhmanabhan et al., 2008). Ignoring the air redistribution phenomenon and non-uniformity in frost growth will result in under predicting the coil capacity.

As the frost grows the coil capacity drops due to decreased air flow rate across the coil and increased resistance to heat transfer due to the low conductivity of the frost layer. Figure 6 shows this drop in capacity for the coil as frost grows. The capacity is presented in dimensionless form using the initial capacity in each case as the normalizing parameter. Capacity degradation in microchannel heat exchangers is fast and almost linear through out the frosting period. This drop in capacity is shown in Figure 6 and it is in agreement with the findings of Shao et al. (2010). If the refrigerant temperature is at -12°C, it takes only 10 minutes to drop the heat transfer rate by 30%. If the glycol temperature is warmer at about -6.7°C, similar heat transfer degradation takes approximately 45 minutes.

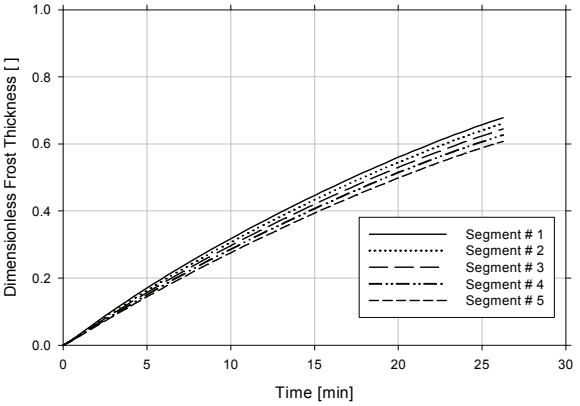

Figure 4: Rate of Frost Growth at Different Segments (-9.4^{0}C EFT, 82% RH and Initial Air Flow Rate of 0.09m^3/s)

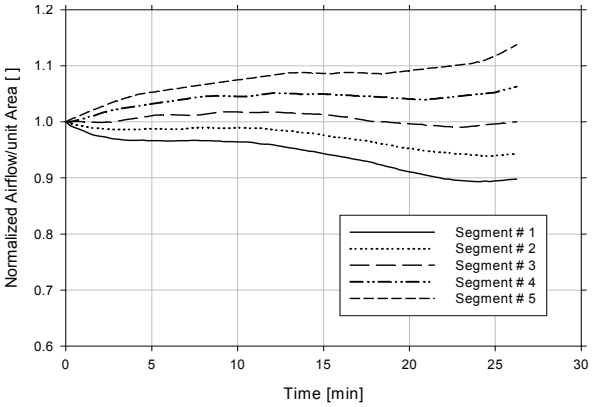

Figure 5: Airflow Rate per unit Area of Segment (Normalized with initial Air flow rate per unit area for that segment)

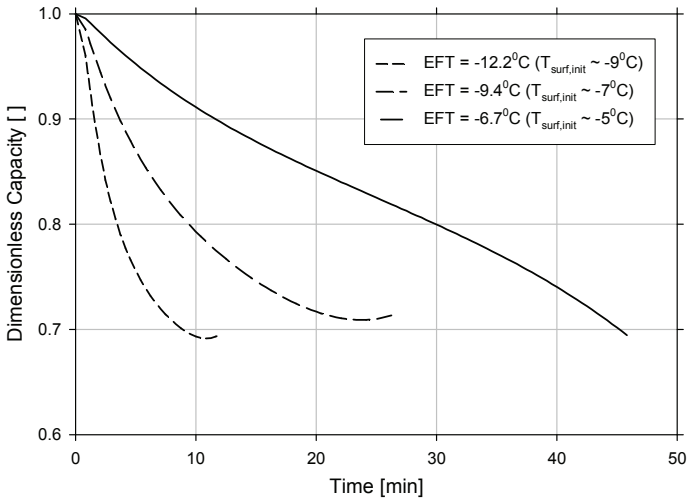

Figure 6: Normalized capacity of the Heat Exchanger during Frosting for Different Entering Glycol Temperatures (Approximate Initial Fin Temperatures shown in parenthesis).

4. CONCLUSIONS

A quasi-steady simulation model based on scaled parameters is presented for analyzing frost growth in microchannel heat exchangers. Condition required for a valid quasi steady state assumption is derived and it is shown that frost growth problem satisfies that condition. The model is incorporated in a segment-by-segment heat exchanger algorithm. Air redistribution due to non-uniform frost growth on the heat exchanger is handled by forcing the pressure drop across each segment to be equal. The simulation results show that the frost growth rate is significantly higher for low temperature case. Frost thickness for different glycol entering temperatures predicted by simulation matched experimental values very well. Model also demonstrated the air redistribution taking place across the segments due to non-uniform frost thickness. Segments with thicker frost see a reduction in mass flux of air, while the redistributed air increases the mass flux in segments with less frost. Microchannel heat exchanger loses capacity faster and almost linearly through out the frosting period. The results of the model are encouraging and suggest that similar models can be used for both conventional fin-tube and microchannel heat exchangers by correctly accounting for heat transfer correlations and air redistribution calculations. The usefulness of the model can be improved by incorporating the ability to predict the variation in frost density along the direction of flow.

NOMENCLATURE

Symbol	Description	Units	Subscripts	Description

A	Area	m^2	fs	Frost surface
D_{AB}	Binary Diffusion Coeff.	m^2/s	f	Frost
h	Heat Transfer Coefficient	W/m^2-K	fl	Fluid
h_m	Mass Transfer Coefficient	m/s	s	Fin/Tube Surface
h_{sg}	Heat of Sublimation	J/kg	sat	Saturated
Ja	Jakob number	-	tp	Triple point
K	Conductivity	W/m-K	v	Vapor
$\dot{m}$	Mass Flow Rate	Kg/s	∞	Air
$\dot{Q}$	Heat Transfer Rate	W		
R	Individual Gas Constant	J/kg- K		
S_f	Half Fin Spacing	m		
T	Temperature	K		
t	Time			
Greek Symbols				
δ	Thickness	m		
ρ	Denisty	kg/m^3		

REFERENCES

Ehsan Moallem., Lorenzo Cremaschi., Daniel Fisher., 2010. Experimental Investigation of Frost Growth on Microchannel Heat Exchangers. Submitted for *Proceedings of 13th Int. Refrigeration and Air Conditioning Conference at Purdue*. West Lafayette, IN, USA, Paper # R2416

Hayashi, Y., Aoki, A., Adachi, S. and Hori, K. 1977. Study of frost properties correlating with frost formation types. *Journal of heat transfer* 99(2), p. 239-245.

Kim, M-H., Bullard, C. W., 2002. Air-side performance of brazed aluminum heat exchangers under dehumidifying conditions. *International Journal of Refrigeration* 25(7), p. 924-934

Kim, J. H., Groll, E.A., 2003. Performance comparisons of a unitary split system using microchannel and fin-tube outdoor coils. *ASHRAE Transactions*, 109(2), p. 219-229.

Kondepudi, S. K., O'Neal, D., 1993. Effects Performance of finned-tube heat exchangers under frosting conditions: I. Simulation model. *International Journal of Refrigeration* 16(3), p. 175-180.

O'Neal, D. L., 1982. The Effect of Frost Formation on the Performance of Parallel Plate Heat Exchanger, PhD Thesis, Purdue University.

S. Padhmanabhan, D. E. Fisher, L. Cremaschi, and J. Knight, 2008. Comparison of Frost and Defrost Performance between Microchannel Coil and Fin-and-Tube Coil for Heat Pump Systems, *Proceedings of 12th Int. Refrigeration and Air Conditioning Conference at Purdue*, West Lafayette, IN, USA, Paper # R2202.

S. Padhmanabhan, D. Fisher and L. Cremaschi, 2010. A Scaling Approach for Predicting Frost Growth in a Heat Exchanger – Application to Fin-Tube Coil, *Proceedings of ASME-ATI-UIT 2010 Conference on Thermal and Environmental Issues in Energy Systems*, Sorrento, Italy (in press).

Shao, L, L., Yang, L., Zhang, C-L., 2010. Comparison of heat pump performance using fin-and-tube and microchannel heat exchangers under frost conditions. *Applied Energy* 87(4). p. 1187 - 1197

Storey, B. D. and Jacobi, A. M., 1999. The Effect of Streamwise Vortices on the Frost Growth Rate in Developing Laminar Channel Flows. *International Journal of Heat Mass Transfer*. 42, p. 3787-3802.

Van Dusen. 1929. International Critical Tables of Numerical Data, Physics, Chemistry and Technology.

Xia, Y., Zhong, Y., Hrnjak, P.S., Jacobi, A.M., 2006. Frost, defrost, and refrost and its impact on the air-side thermal-hydraulic performance of louvered-fin, flat-tube heat exchangers. *International Journal of Refrigeration* 29(7), p. 1066-1079.

Yan, W-M., Li, H-Y., Wu, Y-J., Lin, J-Y., Chang, W-R., 2003. Performance of finned tube heat exchangers operating under frosting conditions. *International Journal of Heat and Mass Transfer* 46(5), p: 871-877

Yang, D-K., Lee, K-S., Song, S., 2006. Modeling for predicting frosting behavior of a fin-tube heat exchanger. *International Journal of Heat and Mass Transfer* 49(7), p. 1472-1479

ACKNOWLEDGEMENTS

The authors would like to gratefully acknowledge the funding and support from the Oklahoma Center for Advancement of Science & Technology and Building Efficiency Division of Johnson Control Inc.